Dynamic Analysis of Fluid – Structure Interaction of Axial Fan System

Dr. Assim Hameed Yousif
Professor
Mechanical Engineering Department-University of Technology
E-mail: assim_yousif20000@yahoo.com

Dr. Wafa Abd Soud Aljanabi
Instructor
Mechanical Engineering Department-UOT
E-mail: wafaabd_92@yahoo.com

Ali Mohammedridha Mahdi
Researcher
Mechanical Engineering Department-University of Technology
E-mail: alimohiraq@yahoo.com

ABSTRACT

Fluid-structure interaction method is performed to predict the dynamic characteristics of axial fan system. A fluid-structure interface physical environment method (monolithic method) is used to couple the fluid flow solver with the structural solver. The integration of the three-dimensional Navier-Stokes equations is performed in the time Doman, simultaneously to the integration of the three dimensional structural model. The aerodynamic loads are transfer from the flow to structure and the coupling step is repeated within each time step, until the flow solution and the structural solution have converged to yield a coupled solution of the aeroelastic set of equations. Finite element method is applied to solve numerically the Navier-Stockes equations coupled with the structural equations The first ten eigenvalue (natural frequency), the first ten eigenvector (mode shape) and effective stress for each part of a rotor system and complete system assembly are predicted.

The validity of the predicted dynamic characteristics of duct fan system was confirmed experimentally by investigating geometrically similar fan system test rig. Good agreement of dynamic characteristics is observed between experimental and numerical results.

Key words: dynamic, fluid-structure interaction, coupling strategies, fan system, natural frequency and mode shape.

تحليل ديناميكي لتداخل المائع والهيكل لمنظومة مروحة محورية

د. عاصم حميد يوسف
أستاذ
قسم الهندسة الميكانيكية - الجامعة التكنولوجية

د. وفاء عبد سعود الجنابي
مدرس
قسم الهندسة الميكانيكية - الجامعة التكنولوجية

علي محمد رضا مهدي
الباحث
قسم الهندسة الميكانيكية - الجامعة التكنولوجية

الخلاصة

استخدمت طريقة تداخل جريان المائع والهيكل للتنبؤ عن المزايا الديناميكية لمنظومة مروحة محورية. تم ربط الحلول العددية لجريان المائع مع الحلول العددية للهيكل باستخدام طريقة البيئة الفيزيائية لتداخل المائع والهيكل.(monolithic method) تم ربط حلول معادلات نفير-ستوك التكاملية ثلاثية البعد مع حلول معادلات الهيكل التكاملية ثلاثية البعد باستخدام طريقة الزمن الحدي. لقد تم نقل الأحمال الديناهوائية من جريان المائع إلى الهيكل وتم إعادة هذه الخطوة المزدوجة مرارا وتكرارا حتى يحصل

الالتئام الكامل لحلول معادلات الجريان ومعادلات الهيكل والذي يقود إلى حلول لمجموعة معادلات المرونة الفضائية. لقد استخدمت طريقة العناصر المحددة لإجراء الحل العددي بشكل مزدوج لمعادلات (نفير-ستوك) التي تحكم المائع مع معادلات تحليل الهيكل. كما استخدمت برامجيات جاهزة لتشغيل طريقة العناصر المحددة وأجراء التحليلات المطلوبة. تم اجراء تحليل ديناميكي لأول عشرة ترددات طبيعية وأول عشرة إشكال نسقيه كذلك الاجهادات الفعالة لأجزاء المنظومة الرئيسية منفردة وللمنظومة مجتمعة.

إن المزايا الديناميكية لمنظومة المروحة التي تم التنبؤ عنها عدديا جرى التأكد من مصداقيتها تجريبا بإجراء اختبارات عملية على منصة فحص يحاكي شكلها الهندسي نموذج الاختبار العددي لمنظومة مجرى المروحة. ولقد لوحظ إن هناك توافق جيد بين نتائج التنبؤ ونتائج القياسات التجريبية للمزايا الديناميكية للمنظومة.

1. INTRODUCTION

The implementation of a coupled problem (fluid-structure interaction) can be done by using two different strategies, which are the monolithic methods and the partitioned method. In a monolithic method, the discretized fluid-structure system is solved together with the mesh movement system in a single iteration loop, leading to a very large system of nonlinear equations to be solved simultaneously. Some advantages of this method are that it ensures stability and convergence of the whole coupled problem. On the contrary, in simultaneous solution procedures the time step has to be equal for all subsystems, which may be inefficient if different time scales are presented for the problem. An important disadvantage is the considerable high computing time effort required to solve each algebraic system and sometimes the necessity to develop new software and solution methods for the coupling method. A monolithic approach to fluid-structure interaction (FSI) used in the present work is introduced by **Hübner, et al., 2004**.

2. TEST RIG

The experimental test rig designed and manufactured according to the requirement of the present study and its consists of driven motor, static frequency changers, spool shaft, fan, two journal bearing, hollow shaft, eight probes, inlet bow mouth, mesh screen and duct casing. The photograph of the test rig assembly and measuring instruments are shown in **Fig. 1**.

The spooled shaft is made from medium carbon steel (St 60.2), with tensile strength of (600 – 720) N/mm², density (7840) Kg/m^3, Young modulus (210) GN/m^2, modulus of elasticity (80) GN/m^2 and length (544.66) mm with step diameters along its length as shown in **Fig. 2**.

The purpose of using two bearings is to support the load to allow the relative motion being smoothly between two elements of machine, made from porosity bronze alloy. Small holes (2 mm) diameter are made into the bush to allow lubricant oil to pass between shafts and bush bearing to lubricate the contact region and reduce temperature rise. The journal bearing oil film may be idealized into stiffness and damping coefficients which affect the flexibility of the system and introduce damping. The viscosity of the lubricant prevents journal bearing from escaping until pressure is built up in the convergent–divergent film, forcing the lubricant oil to escape and at the same time supporting the load across the film. The load capacity is dependent on the viscosity of the lubricant oil type (SAE. 40) was used as recommended by **Aljanabi, 2007**, in which gave the best dynamic performance.

Two house bearings (bed stall) made from iron (CK 45) there outer diameter is (112.2 mm) and inner diameter is (54 mm). House bearing is used to fix the fan system on test rig stand.

The fan used at present test rig has seven blades (aerofoil section of the blades is NACA 5309), each blade span is (114.35) mm, root chord is (86.64) mm, tip chord (46) mm, and maximum thickness of blade is (6) mm, which is located at 30 % from the leading edge and the leading edge blade twist angle is (10º). The stagger angles of the fan blades can be changed during the test

program between (0) to (70º). The fan blades stagger angles are set at (35º) as discovered during the experimental investigation of **Aljanabi, 2007** that give high air speed and uniform flow.

Fine mesh screen fixed behind the fan to smoothing the flow and to minimize the downstream swirls generated by fan rotation.

Hollow shaft has cylindrical shape made from sheet metal (CK 45) has inner diameter (112.2) mm and outer diameter (130.6) mm. Hollow shaft is used to cover the house bearings and to achieve uniform flow of air in the duct test section.

Eight probes were made from (GG18). First four probes are located downstream at a distance (64.14) mm from the fan and the second four probes are located ahead downstream at a distance (415.01) mm from fan, each probe width is (39) mm, thickness is (3) mm and length is (137.7) mm.

Figure 3 shows the schematic diagram of the fan system assembly. The system is isolated in Y-direction from stand frame and ground by four rubber dampers.

AC motor (1.5 KW–50 Hz–3ph) was used to driven the fan system. The motor rotational speed was controlled by using static frequency changer type Hyundai N100.

3. MEASURING INSTRUMENTS

The measuring instruments are flow and dynamic instruments, flow instruments are (Pitot-static tube and micro-manometer), which they used to measure the air flow velocities with respect to the fan rotational speeds. The air velocity obtained for each rotational speed is used as initial input data to the CFD code. Dynamic instruments (accelerometers, vibration transmitters, multiplexer) are also used to measure system dynamic characteristics. Two profile piezoelectric accelerometers (professional vibration sensor), model VB1A4 made by Lutron are used to measure the acceleration and velocity in axial (X) and radial (Y) directions. Two vibration transmitters model TR-VBT1A4 made by Lotrun are used as sensors controller which supply electricity current to excite the sensors in the same time work as an integral circuit that convert the output analog signal (4-20) mv to digital signal. A multiplexor is used to allow the digital signals of two sensors to be record in the same time as sixty reading per second each one. The digital signal then supplied to personal computer. A visual studio program is prepared to represent the output data and to make the analysis required. Data acquisition system was used with a widows-base PC and communication between electrical accelerometers sensor, hardware (card interface), and PC was controlled via software written in Visual studio. The interface precedes raw data transmitted from sensor. Then raw data are digitalized and passed through amplifier to magnify signal before the receiver calculated the time average of the measuring data.

SBS Portable Balancer (SB-1700) is used to permit quick measurements of balance level for various fan system rotational frequency. Laser tachometer (included with the SBS Portable Balance) is used to calibrate the speed indicator of the frequency changer and to check the preciosity of the piezoelectric accelerometers reading.

4. VIBRATION ANALYSIS USING FINITE ELEMENT SIMULATIONS

In the present study the general guideline of the finite element analysis follows the steps described by **Mehdizadeh, et al. 2008**. When finite element method (FEM) applied the solution of eigenvalue, the algebraic eigenvalue problem is exist. Symmetric matrices of order (n) are used as

given by **Nakasone, et al. 2006** to fix up the problem. Finite element method also applied to fix the eigenvector problem. Structural systems are very often subjected to transient excitation. A transient excitation is a highly dynamic, time-dependent force exerted on the solid or structure, **Entwistle**, **2001**. Time stepping used in finite difference methods are employed in solving transient problems.

Finite element method was tested and extensively developed for structural and solid mechanics problems; it was not admitted as a powerful tool for the solution of fluid mechanics problems until recently reported by **Nakasone, et al. 2006**. The basic concepts associated with the application of the FEM to solve problems in fluid mechanics are summarized in the idealized block diagram given by **Lie,** and **Quek, 2003**. The flow assumed to be three dimensional, steady, incompressible and Newtonian when passing the hollow shaft. The boundary conditions for the problem are specified in terms of pressure and velocity.

5. FLUID–STRUCTURE INTERFACE

Fluid–structure coupled computation is performed by solving the Navier-Stokes equation coupled with the structural equation. The coupled fluid-structure equation is obtained as given by **Vad, et al., 2001,** as follows in Eq. (1) and Eq. (2):

FEM for Structure $$[K_S]\{\delta\} + [M_S]\{\ddot{\delta}\} - [A]^t\{P\} = \{F\} \quad (1)$$

FEM for Fluid $$[K_f]\{P\} + [A]\{\ddot{\delta}\} = 0 \quad (2)$$

For free vibration, the coupled fluid-structure equation is given in Eq. (3):

$$\begin{bmatrix} M_S & 0 \\ A & 0 \end{bmatrix} \begin{Bmatrix} \ddot{\delta} \\ \ddot{P} \end{Bmatrix} + \begin{bmatrix} K_S & -A^t \\ 0 & K_f \end{bmatrix} \begin{Bmatrix} \delta \\ P \end{Bmatrix} = 0 \quad (3)$$

6. NUMERICAL SIMULATION

Soft ware package ANSYS is used to run the finite element method and to make the analysis required. The main complete flow chart for the numerical simulation as given by **Mohammed, 2007** is introduced to do the reprocess step (read geometry and material data, boundary conditions and initial conditions of the problem), to do the processor step (generate finite element mesh, calculate element matrices, assemble element equation and solve the equation) and to do the postprocessors step (compute the solution and it's derivative at desired paints of the domain and print/plot the result). In the case study analysis for axial fan system all solution is linear except the contact region between shaft and fan.

Air flow load which applied on hollow shaft are non-linear solution. It is essentially the preprocessing is the same for both linear and non-linear analysis, although non-linear analysis might include special elements and non-linear material properties. ANSYS will automatically generate all the nodes and the elements, by specifying:

1- Element attributes include element types, real constants, and material properties.
2- Element size controls the fineness of the mesh.

The next step of finite element analysis involves applying appropriate boundary conditions and the proper loading. The ways used to apply boundary conditions is the same as they used by **Antunes, et al., 2005**.

In this step, the analysis type is defined (static load, transient applies loads, specifying load steps and initiates the finite element solution).

A non–linear analysis will differ from a linear solution in that it often requires load increments and always requires equilibrium iteration. In present study a non-linear static analysis is applied, with convergence criteria, incremental load and specified load step. The main goal of the finite element analysis here is to examine how a structure or component responds to certain loading conditions. The solution of non-linear problems by finite element method is usually attempted by basic techniques given by **Hassan, 2007**.

7. COUPLED-PHYSICS ANALYSIS

When the fluid flowing over a hollow shaft provides pressure loads that can be used in the structural analysis. The pressure loading is a result in a deflection of the hollow shaft. This deflection, in principle, changes the geometry of the flow field around the hollow shaft, but in practice, the change is very small enough and may be regarded to be negligible. Thus, there is no need to iteration. In this problem, fluid element is used for the flow solution and structural elements for the stress and deflection calculations.

ANSYS program performs load transfer coupled the physics analysis by using the concept of a physics environment. The term physics environment applies to both files created which contains all operating parameters and characteristics for a particular physics analysis and to the file's contents. The data used in the present physics environment method are a single data base and multiplies physics environments as represented by **Daneshmand, 2000**, in which he build a model encompassing all physics requirement. He assign attribute to the model and create physics environment to be used in the analysis. The method starts with (step one) solving the first physics environment, then step two is done with solving next physics environment. The next step is done by solving the current physics environment with the couple-field loads. At last more physics environment are solved, or feedback coupling to physics environment of step two. This feedback close loop is repeated many times until the solution is obtained.

8. MODEL GENERATIONS

The model generations procedure is presented for dynamic modeling of axial fan (rotor-bearing system) by using solid modeling approach method represent by ANSYS drawing key point. Bearing is representing in ANSYS-11 software by using direct generation method, it represent by element COMBIN14 (Combination of spring and damper). The stiffness value of the journal bearings is taken as calculated by **Aljanabi, 2007**.

Air flow is expressed by using solid modeling approach method and meshed by using FLUID142 elements. Element type for each system part is listed in **Table 1**.

9. STRUCTURE MODAL ANALYSIS

The results reported here are the first ten of the structural natural frequency (eigenvalue) and mode shapes (eigenmodes) based upon the behavior of each part of the system (shaft, fan and hollow shaft).

Fig. 4 shows the numerical results of the ten first mode shape of the shaft. The modes titled numbers 1 and 2 show the harmonic motion of the shaft in radial (Y)-direction. These two modes indicated that the oscillatory motion is a function of sine and cosine waves. While mode number 4 shows the shaft oscillatory motion in Z-direction. Modes number 5 and 9 show the transverse vibration in which the shaft is extended and bended, this type of vibration motion indicated that the shaft effected by bending stresses. Modes number 3, 7 and 8 show the torsion vibration in which the shaft is under the influence of the torsion stress. While mode number 6 shows that the shaft is under the torsion vibration and simple harmonic motion (i.e. the shaft is rotate with oscillatory motion in Z-direction). Mode number 10 shows the torsion-transverse vibration due to shaft rotation and the vibration motion appeared to be perpendicular to the shaft axis.

Fig. 5 shows the modal analysis used to determine natural frequency of the fan. Modes number 1, 2, 3, 4, 5, 6 and 7 show that the blades are under the influence of bending, while mode number 8 shows that the fan is under the influence of the torsion and bending together. Mode numbers 9 and 10 showed that the blades are under the influence of twist. As seen in these modes the variation of degrees of freedom is exited in each vibration mode. This may is due to the results of a direct coupling consequence between the degree of freedom in which this explanation is also given by **Ranwala, 2009**. Since blades have to rotate, it must have a lightweight structure as in the present fan, which resulting in their reduced stiffness when compared with other part of a rotor system. Hence blades are quite flexible and can easily bend and twist under the influence of air loads. Although the static air loads on the blades being to twist and bend in a periodic manner, under certain conditions the dynamic air loads may being feeding the elastic motion of the blades, causing its amplitude to grow, which in turn causes increased air loads that eventually exceed the fan strength. Such a catastrophic dynamic coupling between the elastic motion and aerodynamic loading is called flutter. This statement is also in some way has been reported by **Dettmor, 2004**.

Fig.6 shows the first ten mode shape of the hollow shaft. Mode numbers 3, 4, 6 and 7 show that the hollow shaft is vibrated longitudinally in which it is extended and constricted in axial direction. This type of vibration leads to tensile and compressive stresses. Mode numbers 1, 2, 8 and 9 show that the hollow shaft vibrated in transverse direction in which it is extended and bended. This type of vibration is leads to bending stresses. Mode numbers 5 and 10 show torsion vibration in which the hollow shaft is under the influence of the torsion stress.

It can be noticed that the natural frequency for each part of a rotor system was increased with increase of mode number starting from mode number 1 up to mode number 10. The average of the percentage rate of natural frequency is increased for shaft by 44.5%, for fan by 27.32% and for hollow shaft by 12.455%. The highest values of the natural frequency is recorded at shaft and decreased gradually for hollow shaft and fan respectively.

10. FLUID ANALYSIS

The load on the rotor system depends directly on the flow velocity and pressure, when the pressure increase so does the load. The pressure actually fluctuated on the rotor system as the flow passes from fan to the hollow shaft. Five cases of fluid are investigated in this study with respect to the shaft speed.

Fig. 7 shows the summations of velocity distributions for various rotational speeds at the duct exist. The velocity is increased with the increase of rotational speed. At low rotational speed 500 rpm, the velocity distribution is clearly seems to be fully developed. Some deviation is observed from the fully developed flow at the center of blade when the rotational speed increased, this

deviations may be exists because the blade twist angle is insufficient enough to produce linear blade loading.

The regions close to the hollow shaft is called **(**fluid-structure regions**)** according to remarkable notes given by **Alzafrany, 2006**. **Fig. 8** shows the pressure distribution along the hollow shaft axis passing through the probe region at difference rotational speed. The pressure exerted on the hollow shaft is reduced gradually in the region just behind the fan. When the air flow passed through the first set of probes, pressure is increased to maximum value at the probes stagnation point and then drops when the flow passes the probes surfaces. Between two set of probes, the pressure distributions became constant. At the second set of probes the pressure increased again to high value because the flow is stagnated at the probes leading edges and then drops when the flow passes on probes surfaces.

According to above discussion one may be decide in the experimental investigation to fix the accelerometer sensors at the mid way along hollow shaft axis in the region when the pressure distribution seems to be approximately constant.

11. STATIC ANALYSIS OF FLUID-STRUCTURE INTERACTION

Figures 9, 10, 11, 12 and **13** show that the fan has maximum stress and higher than the other system parts due to the effect of the generation of the centrifugal stresses, in which these stresses are increased with increase of rotational speed.

The stresses generated along the shaft is maximum at region of sudden change of the cross sectional area (i.e. shaft diameters variations), because all stresses are concentrated at this region, while the minimum stress is recorded at the bearing contact region since the bearing support and carried the shaft.

Fan stress records maximum value at blade roots in which the centrifugal force tend to extirpate the blade from root. While the hollow shaft is influenced by the buildup of pressure of flowing air, and this leads to tensile forces which resist the bursting forces developed across longitudinal and transverse directions.

12. TRANSIENT ANALYSIS

Non-synchronous vibration amplitude is analyzed theoretically and experimentally at various rotational speeds. **Figs. 14, 15, 16, 17** and **18** show the amplitude for a rotor system in axial (X) and radial (Y)-directions. It can be seen that the amplitude in the X-direction is higher than that for Y-direction. This may be due to existent of four dampers in Y-direction used to isolate the system from stand and ground interference. The amplitudes in axial (X) and radial (Y) directions are decreases when the rotational speed is increased. The average of amplitude rate is decreased by 47.949 % in axial-direction and by 47.3 % in radial-direction. The percentage errors between the experimental and the theoretical results of the amplitude components in axial (X) and radial (Y) directions are presented in **Tables 2** and **3**. In spite of that good agreement is observed between experimental and numerical amplitude results in axial (X) and radial (Y) directions as shown in **Figs. 19** and **20** respectively.

13. CONCLUSIONS

According to the adopted data and the obtained results, the present work has reached the following conclusions. The coupling strategies problem (fluid-structure interaction) of duct fan system can be overcome (treated and analyzed) numerically by using finite element method

(monolithic method). Experimental investigation of duct fan system satisfied the numerical approach of the coupling problem (fluid-structure interaction). The mode shape depended upon the degree of freedom. The natural frequency for every part of the system and system assembly were increased with increase of mode shape number starting from mode 1 up to 10. Aerodynamic force exerted on the hollow shaft due to air flow is reduced gradually downstream the fan disk of system. The amplitude in axial (X) direction is higher than the amplitude in radial (Y) direction, since the system is isolated in Y-direction from stand frame. The amplitude value decreases when the rotational speed increased.

REFERENCES

- Aljanabi, W. A., 2007, *Theoretical and Experimental Study of an Axial Fan Rotor Bearing System Using Vibration Analysis*, ph. D. Thesis, Mechanical Engineering Department, University of Technology, Baghdad, Iraq.

- Al-Zafrany, A., 2006, *Finite Element Methods*, School of Engineering, Cranfield University, United Kingdom.

- Antunes, A. R., Lyra, P. R., Willmersdorf, R. B., 2005, *A Methodology and Computational System For The Simulation of Fluid-Structure Interaction Problem*, Journal of The Braz. Soc. Of Mech. Sci. and Engineering, Vol. 27, No. 3, PP. 255-265.

- Daneshmand, F., 2000, *Fluid-Structure Interaction Problems and It's Application in Dynamic Analysis*, Ph. D. Thesis, Mechanical Engineering, Shiraz University, Iran.

- Dettmor, W. G., 2004, *Finite Element Modeling of Fluid Flow With Moving Free Surfaces and Interface Including Fluid-Solid Interaction*, Ph. D. Thesis, School of Engineering, University of Wales, United Kingdom.

- Entwistle, K. M., 2001, *Basic Principles of The Finite Element Method*, Alden Press, 1st Published, Oxford, United Kingdom.

- Hassan, A. J., 2007, *Effect of Shape and Location of Cutout on The Dynamic Response of Thin Cylindrical Shell*, M. Sc. Thesis, Nahrain university, collage of engineering, Iraq.

- Hübner, B., Walhorn, E., and Dankler, D., 2004, *A monolithic approach to fluid-structure interaction using space-time finite elements*, Elsevier Journal, Vol. 193, No. 9, PP. 2087-2104.

- Liu, G. R., and Quek, S. S., 2013, *The Finite Element Method: A Practical Course*, Elsevier Butterworth-Heinemann, 2nd Published, Oxford, United Kingdom.

- Mehdizadeh, O. Z., Zhang, C., and Shi, F., 2008, *Flow Induced Vibratory Stress Prediction on Small Turbofan Engine Compressor Vanes Using Fluid-Structure Interaction Analyses*, Alaa Journal, Vol. 4, No. 12, PP. 2431-2483.

- Mohammed, T. F., 2007, *Hot Extrusion with Tilting Dies*, M. Sc thesis, Technical College, Baghdad, Iraq.

- Nakasone, Y., Yoshimoto, S., and Stolarski, T., 2006, *Engineering Analysis With Ansys Software*, Elsevier Butterworth-Heinemann, 1st Published, Oxford, United Kingdom.

- Rangwala, A. S., 2009, *Structural Dynamics of Turbo-machines*, New Age International (p) Ltd., 1st Edition, Delhi, India.

- Vad, J., Bensze, F., Corsini, A., and Pispoli, F., 2001, *Non-Free Vortex Flow Effects in an Axial Flow Rotor*, Periodical Polytechnic Ser. Mech. Eng., Vol.45, No. 2, PP. 201-216.

15. NOTATION

A = fluid-structure interaction matrix.
F = nodal point load vector acting on the structure.
F.E.M = finite element method.
FSI = fluid-structure interaction.
K_f = stiffness matrix of pressure.
K_s = stiffness matrix of the structure.
M_s = mass matrix of the structure.
NACA = the national advisory committee for aeronautics.
P = unknown nodal pressure vector of the fluid.
$\ddot{P}$ = double derivative of nodal pressure after incorporating boundary condition.
X = axial direction.
Y = radial direction.
Z = axis perpendicular to X, Y plane.
δ = unknown nodal displacement vector of the structure.
$\ddot{\delta}$ = normal acceleration vector.
Φ = diameter, mm.

Table 1. Define labeled numbers are as given in **Fig. 3** and element type.

No.	Discription	Element Type
1	Shaft	SOLID72
2	Hollow Shaft	SOLID72
3	Bush Bearing	COMBIN14
4	House Bearing	COMBIN14
5	Teflon	COMBIN14
6	Fan	SOLID72
7	Probe	FLUID142
8	Fluid	FLUID142
9	Fluid-Strucre	FLUID142- SOLID45
10	Circuler Duct	FLUID142

Table 2. Amplitude values and errors in X-direction.

N (rpm)	Experimental Work in X-direction (m)	Theoretical Work in X-direction (m)	% error
500	2.5532E-4	2.43603E-4	- 4.809
1000	6.38323E-5	6.56559E-5	2.7775
1500	3.64756E-5	4.00810E-5	8.995
2000	2.7356E-5	3.2198E-5	15.038
2500	2.626245E-5	2.8358E-5	7.3896

Table 3. Amplitude values and errors in Y-direction.

N (rpm)	Experimental Work in Y-direction (m)	Theoretical Work in Y-direction (m)	% error
500	2.1885E-4	2.118124E-4	- 3.22814
1000	6.38323E-5	6.40657E-5	0.363
1500	3.6475E-5	3.87487E-5	5.8678
2000	2.62168E-5	3.14019E-5	16.515
2500	2.58962E-5	2.9746E-5	12.9422

Figure 1. Photograph of the fan system and measuring instruments**.**

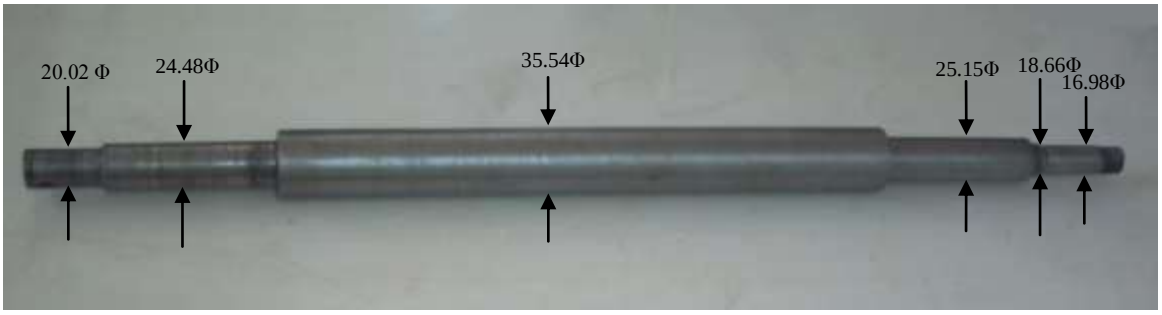

Figure 2. Photograph of the spooled shaft (all dimension in (mm)).

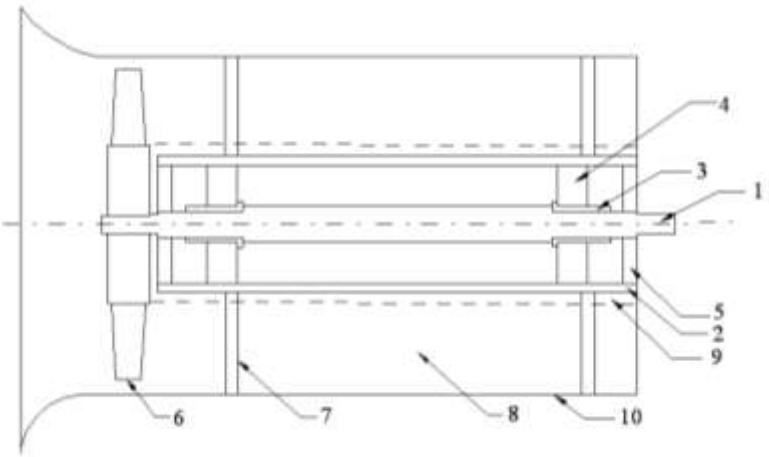

Figure 3. Schematic diagram of the fan system assembly, key of labeled numbers are as given in **Table 1.**

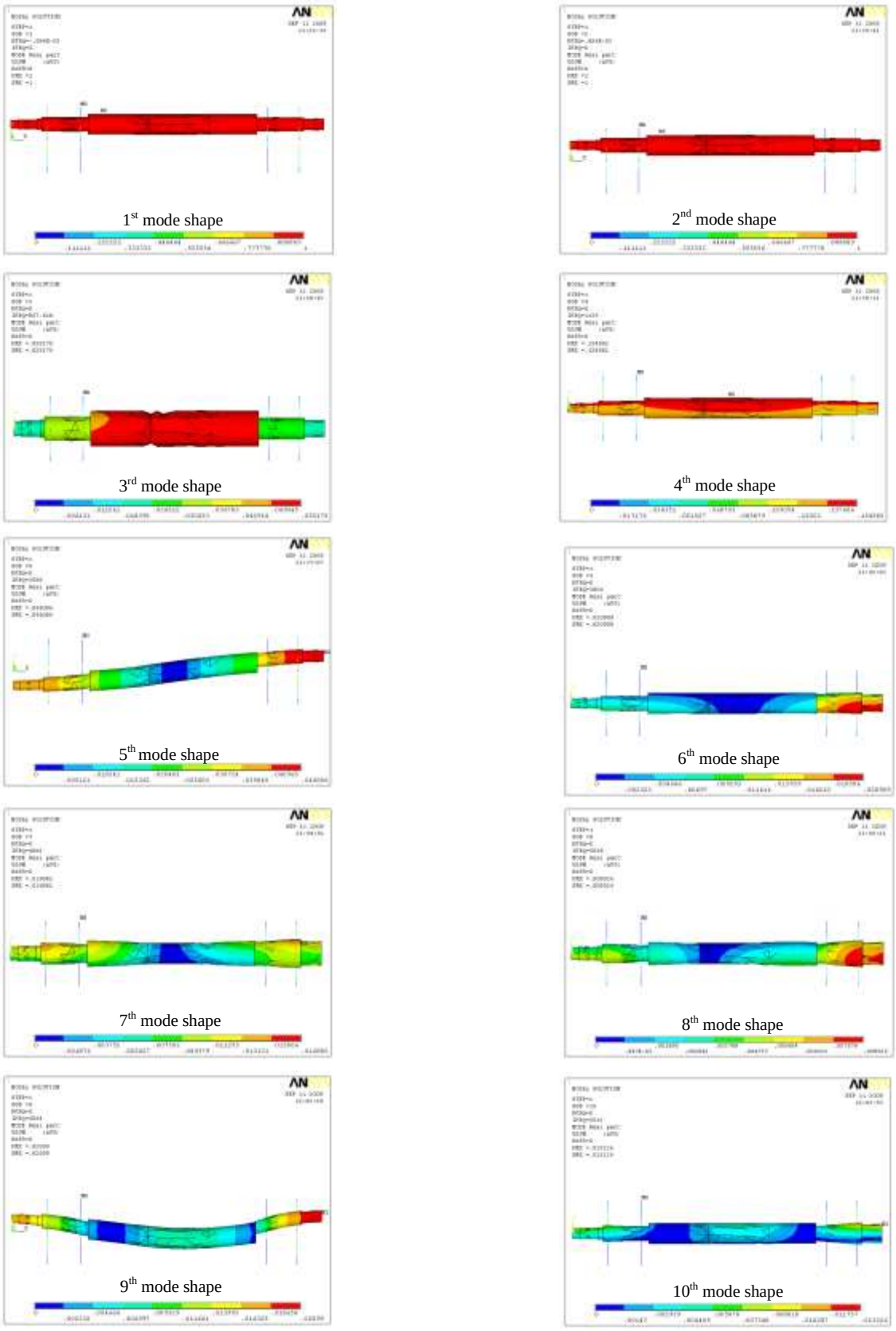

Figure 4. Natural frequency and mode shape for the spooled shaft.

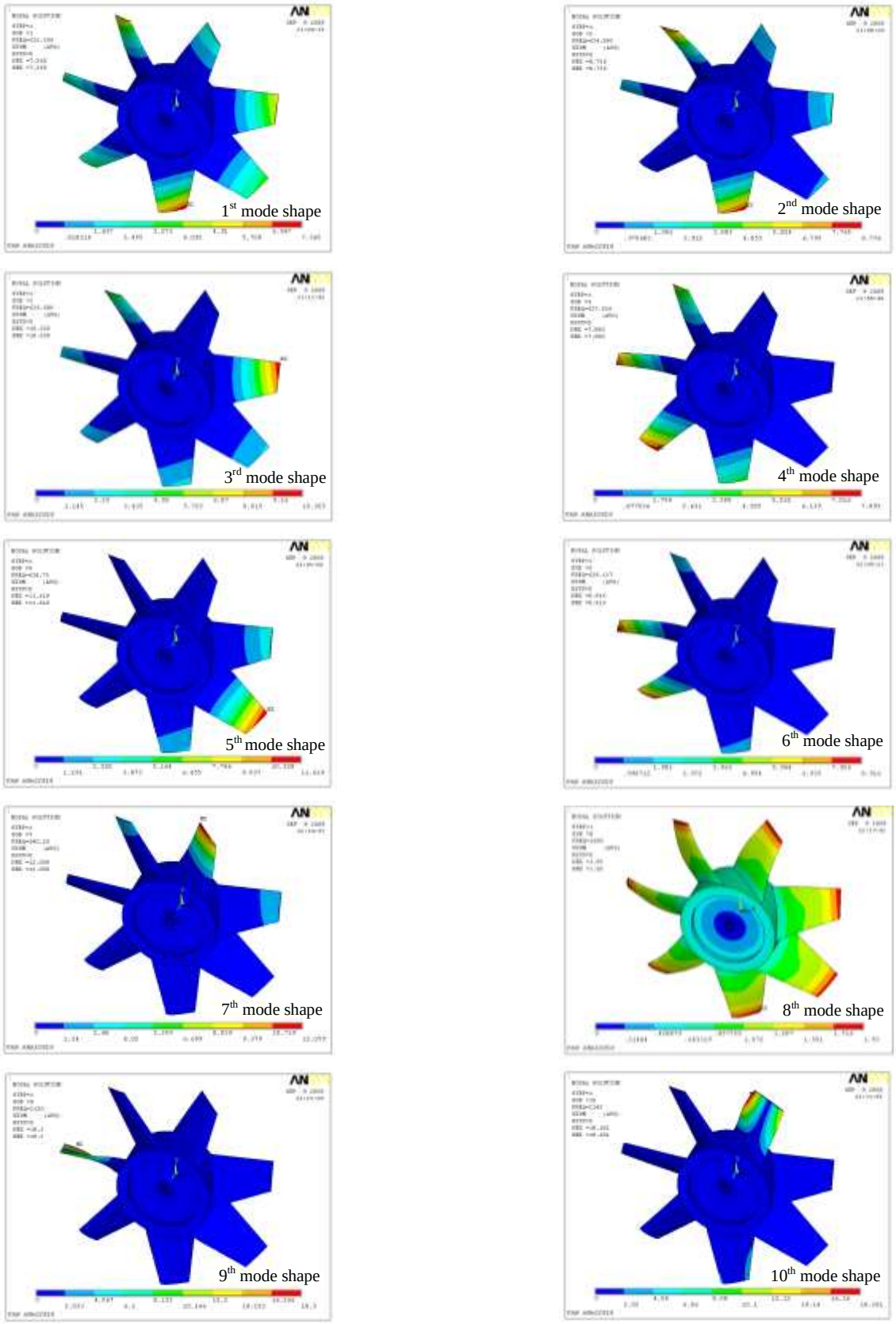

Figure 5. Natural frequency and mode shape for axial fan.

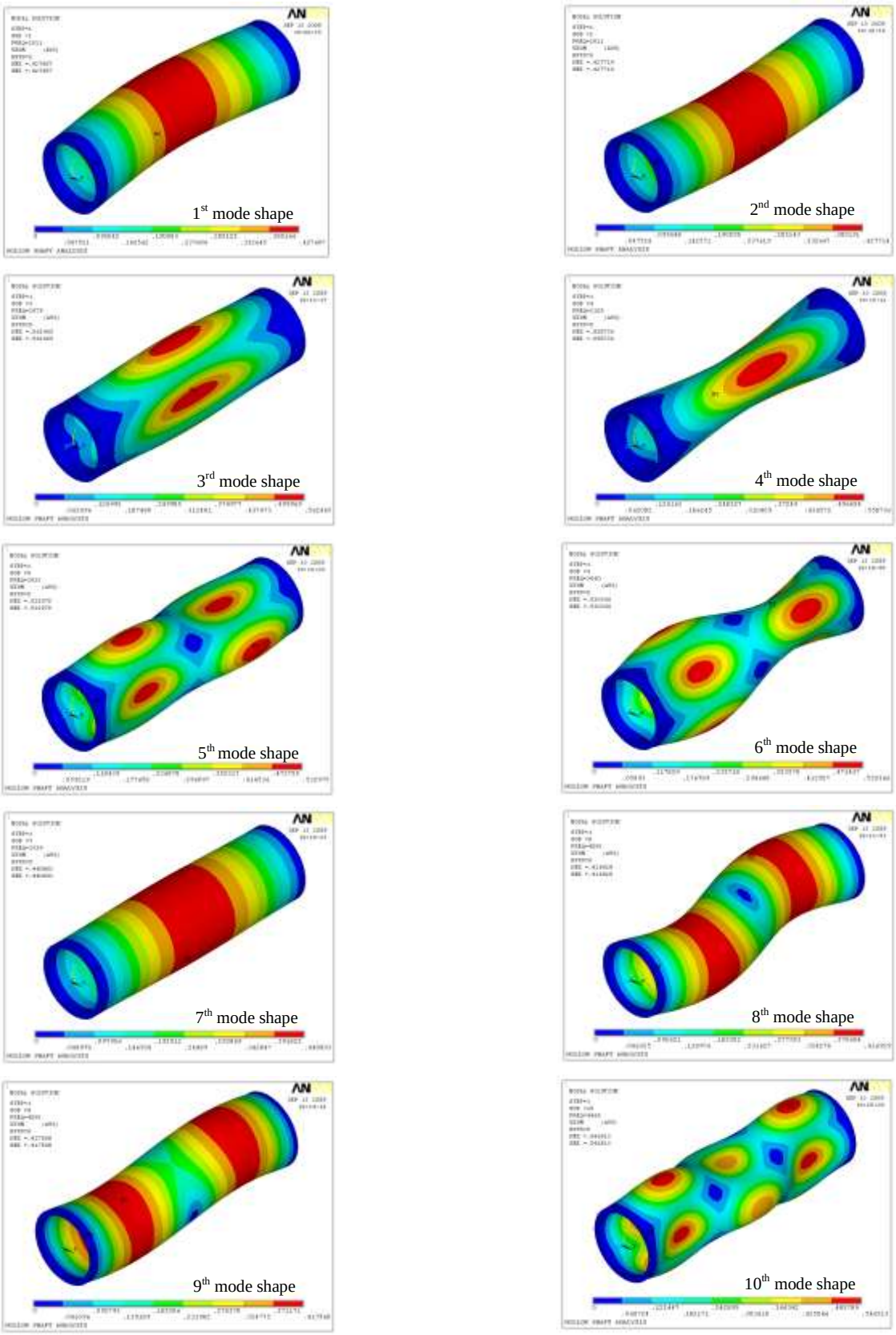

Figure 6. Natural frequency and mode shape for a hollow shaft.

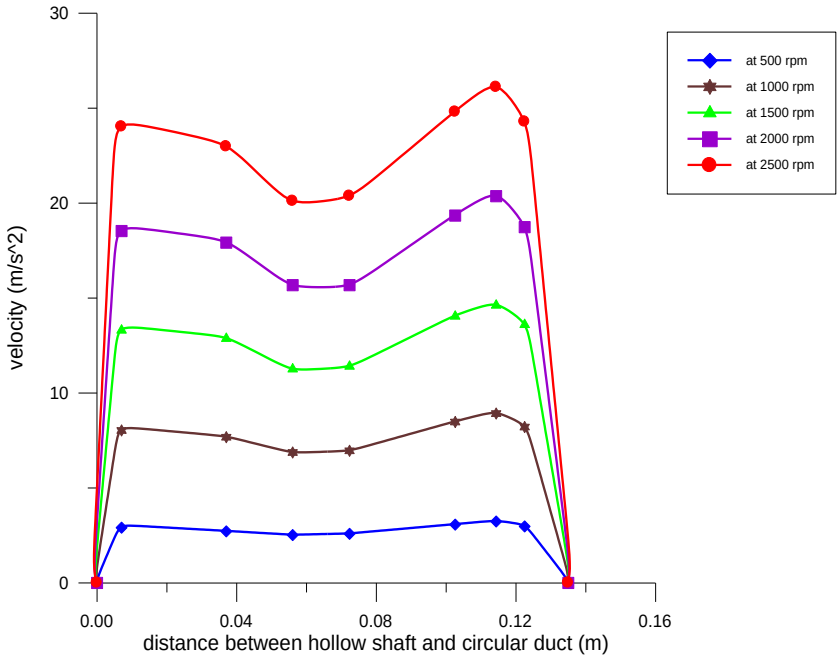

Figure 7. Summation velocity distribution at the outlet of a rotor system at various rotational speeds.

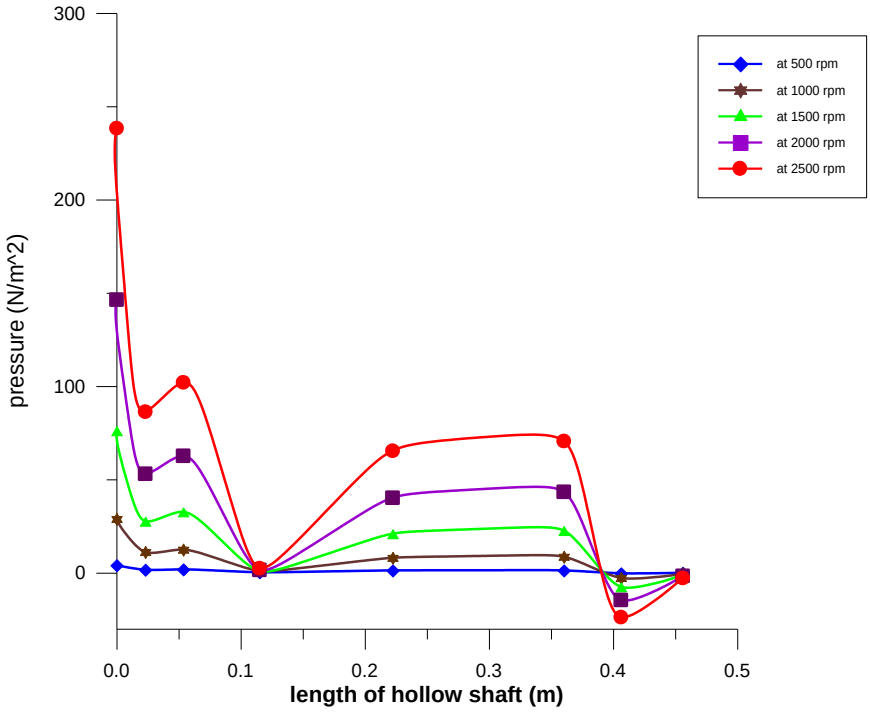

Figure 8. Pressure distribution of fluid-structure interaction at various rotational speeds.

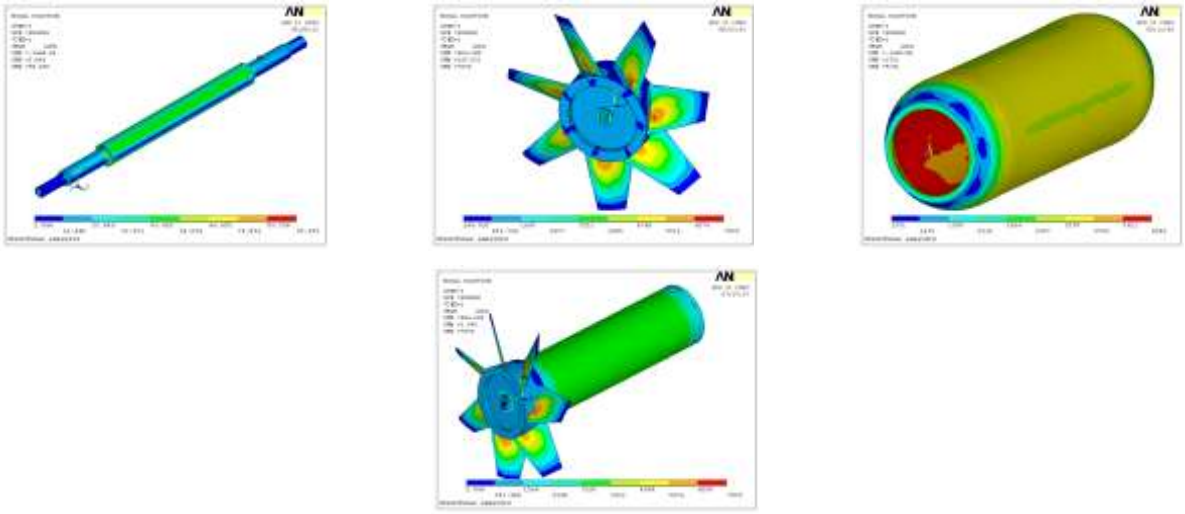

Figure 9. Static stress analysis of system parts and system at rotational speed (500) rpm.

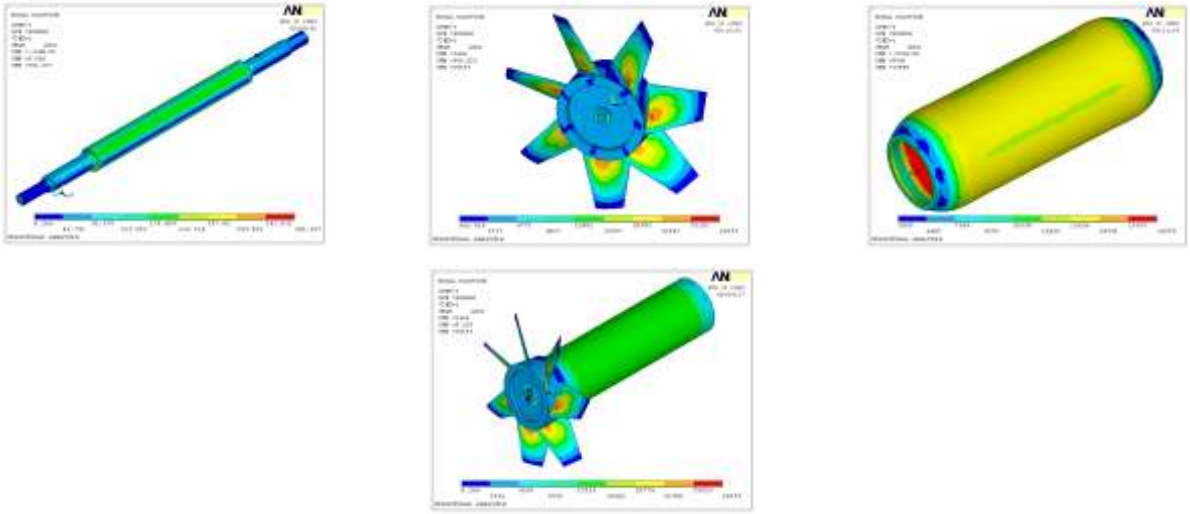

Figure 10. Static stress analysis of system parts and system at rotational speed (1000) rpm.

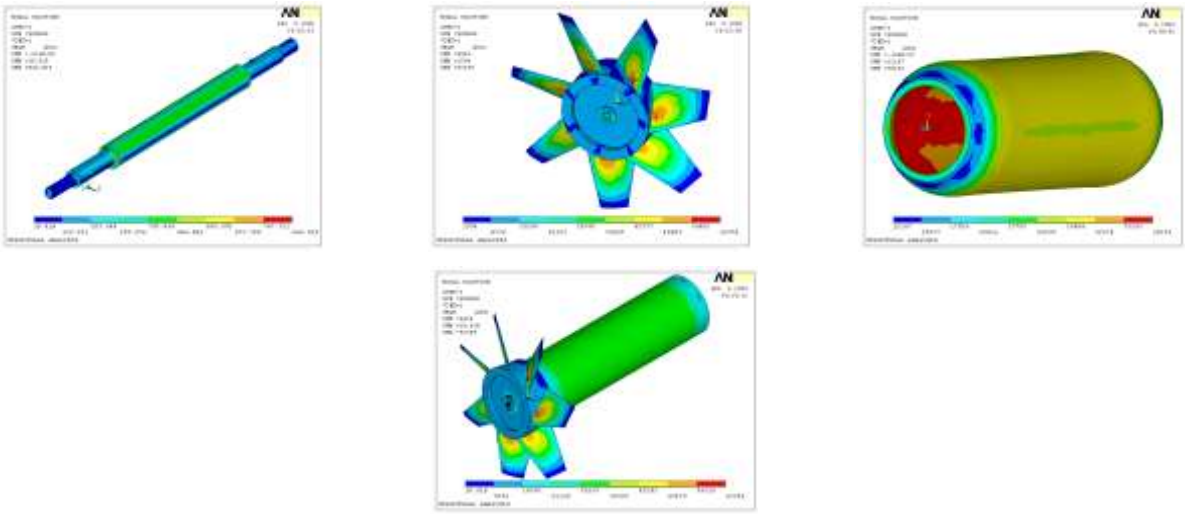

Figure 11. Static stress analysis of system parts and system at rotational speed (1500) rpm.

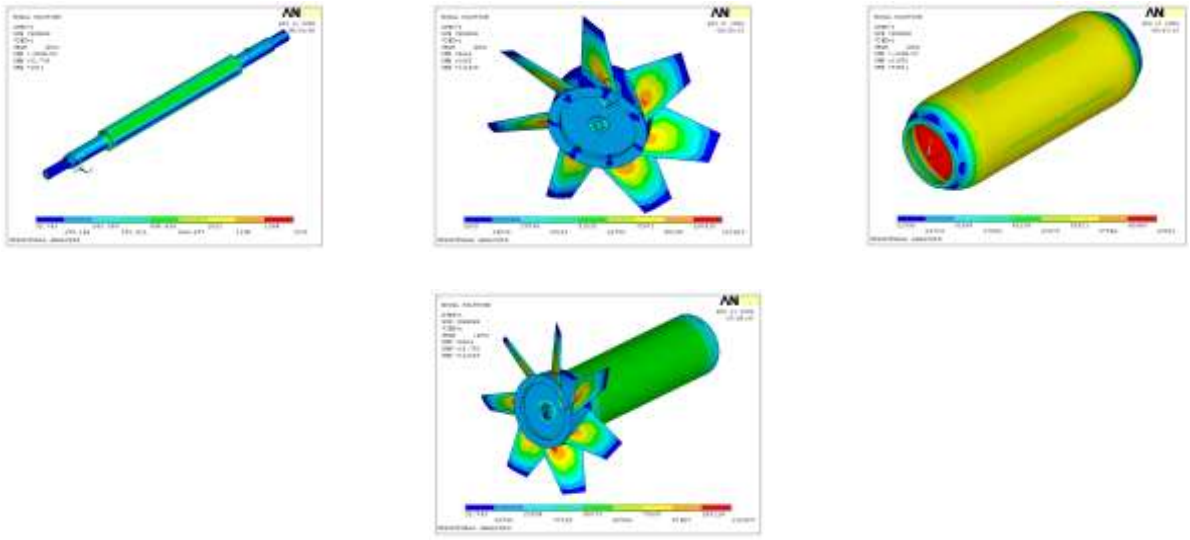

Figure 12. Static stress analysis of system parts and system at rotational speed (2000) rpm.

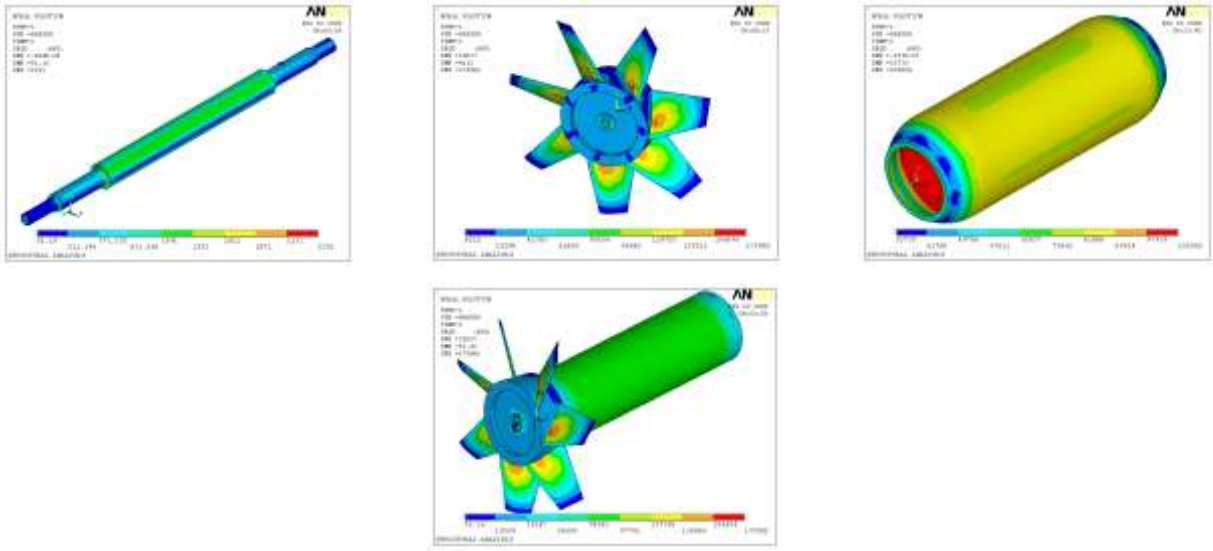

Figure 13. Static stress analysis of system parts and system at rotational speed (2500) rpm.

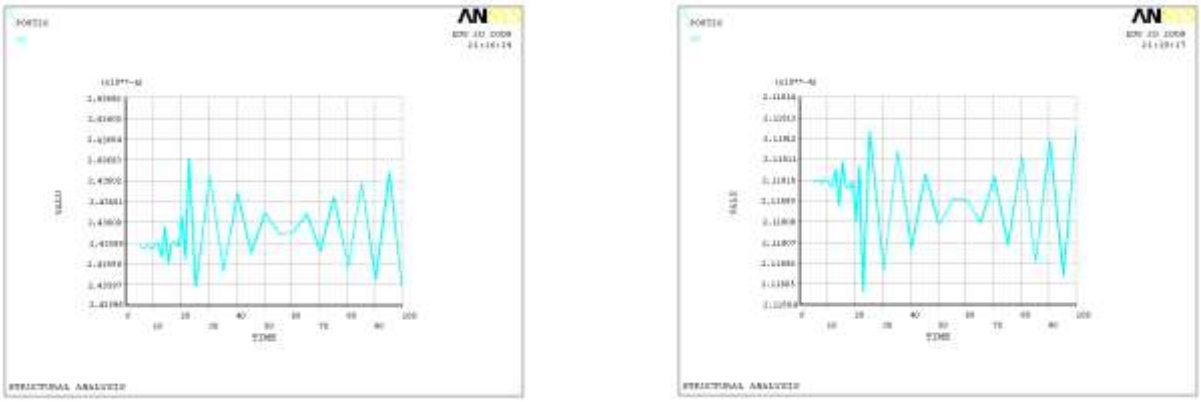

Figure 14. Non-synchronous vibration amplitude for a rotor system in X and Y-directions at (500) rpm.

Figure 15. Non-synchronous vibration amplitude for a rotor system in X and Y-directions at (1000) rpm.

Figure 16. Non-synchronous vibration amplitude for a rotor system in X and Y-directions at (1500) rpm.

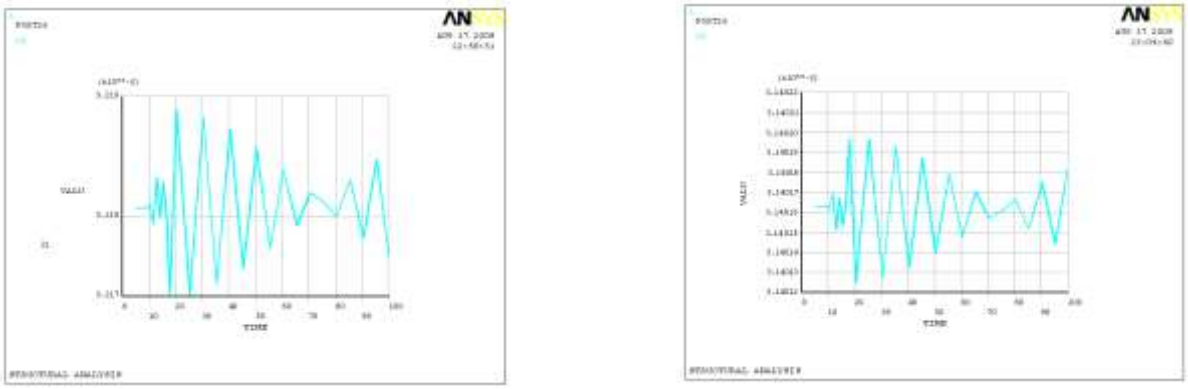

Figure 17. Non-synchronous vibration amplitude for a rotor system in X and Y-directions at (2000) rpm.

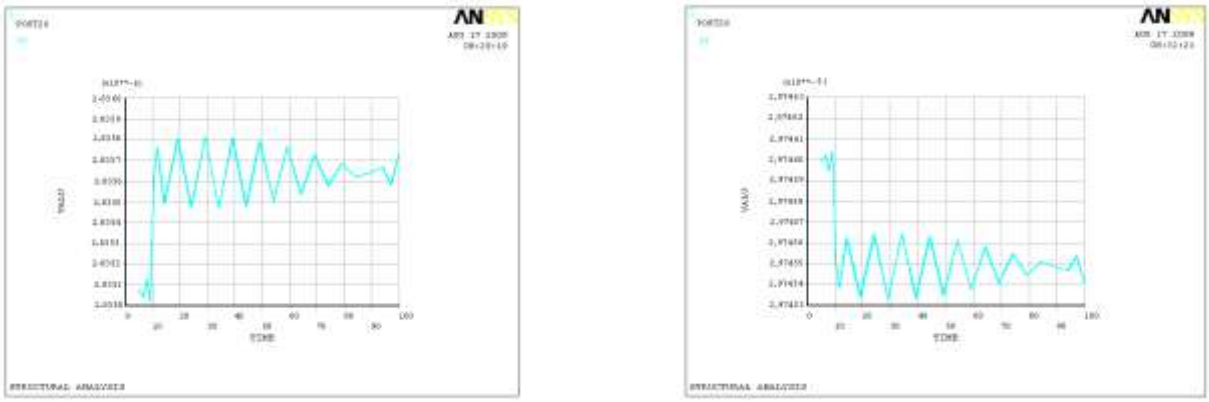

Figure 18. Non-synchronous vibration amplitude for a rotor system in X and Y-directions at (2500) rpm.

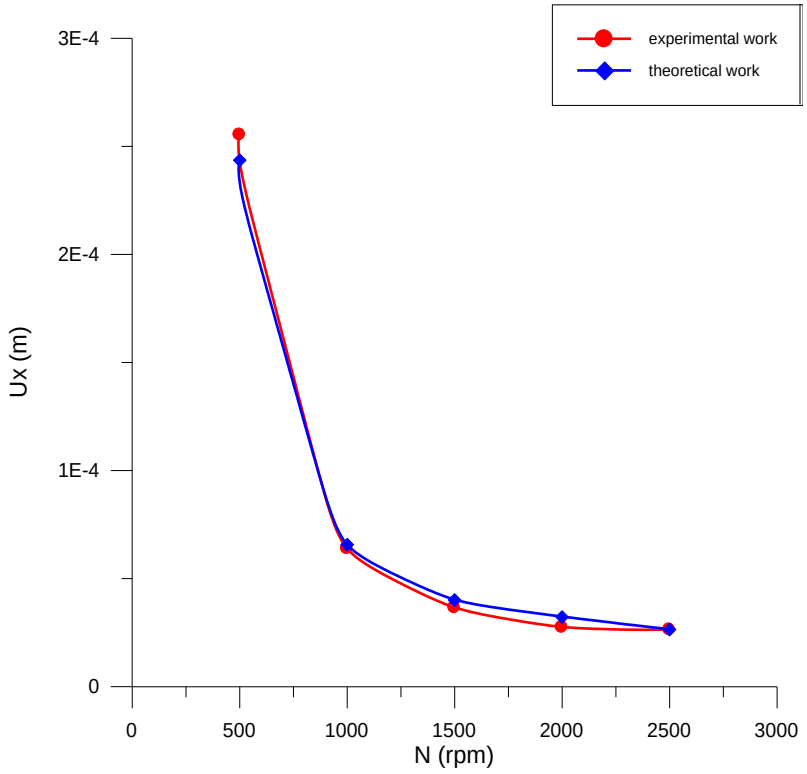

Figure 19. Experimental and theoretical amplitude in X-direction.

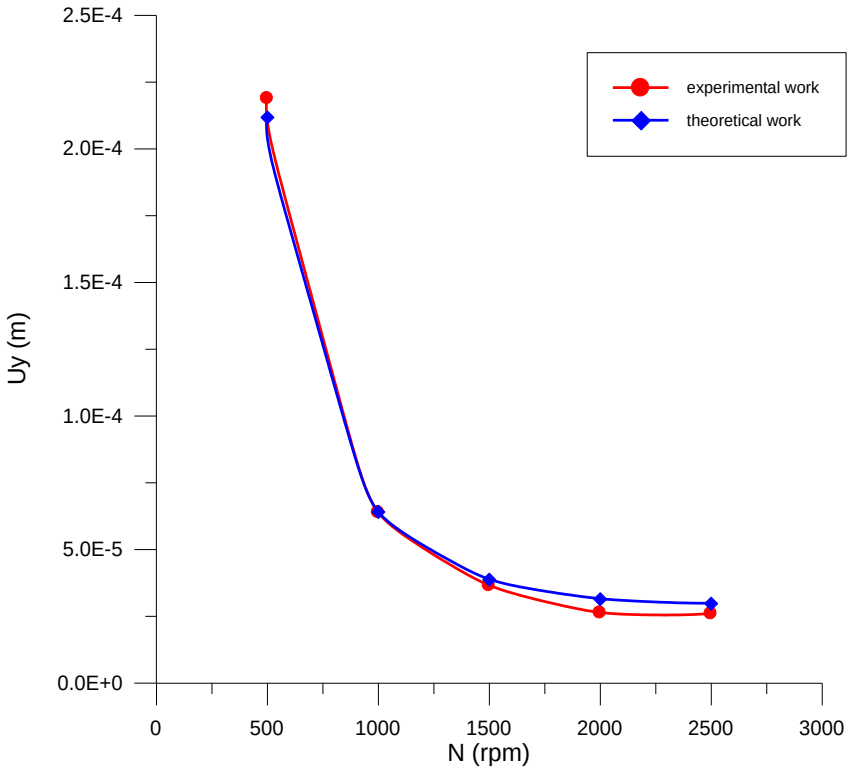

Figure 20. Experimental and theoretical amplitude in Y-direction.